Supporting Information

High-defect hydrophilic carbon cuboids anchored with cobalt/cobalt oxide nanoparticles as highly-efficient and ultra-stable lithium-ion battery anodes

Xiaolei Sun,[a,c] Guang-Ping Hao,[b] Xueyi Lu,[a] Lixia Xi,[d] Bo Liu,[a] Wenping Si,[a] Chuansheng Ma,[e] Qiming Liu,[f] Qiang Zhang,[g] Stefan Kaskel,[b]* and Oliver G. Schmidt [a,c]*

[a] Institute for Integrative Nanosciences, Leibniz Institute for Solid State and Materials Research (IFW Dresden), Helmholtzstrasse 20, Dresden, 01069 Germany.

[b] Department of Inorganic Chemistry, Technische Universität Dresden, Bergstrasse 66, Dresden, 01062 Germany. E-mail: Guang-Ping.Hao@chemie.tu-dresden.de (G. -P. Hao); Stefan.Kaskel@chemie.tu-dresden.de (S. Kaskel)

[c] Material Systems for Nanoelectronics, Technische Universität Chemnitz, Reichenhainer Strasse 70, Chemnitz, 09107 Germany.

[d] Institute for Complex Materials, IFW Dresden, Helmholtzstrasse 20, Dresden, 01069 Germany.

[e] Electronic Materials Research Laboratory, Key Laboratory of the Ministry of Education and International Center for Dielectric Research, Xi'an Jiaotong University, Xi'an, 710049 P.R. China.

[f] Graduate School of Science and Engineering, Saitama University, Saitama, 338-8570 Japan.

[g] Beijing Key Laboratory of Green Chemical Reaction Engineering and Technology, Department of Chemical Engineering, Tsinghua University, Beijing, 100084, P.R. China.

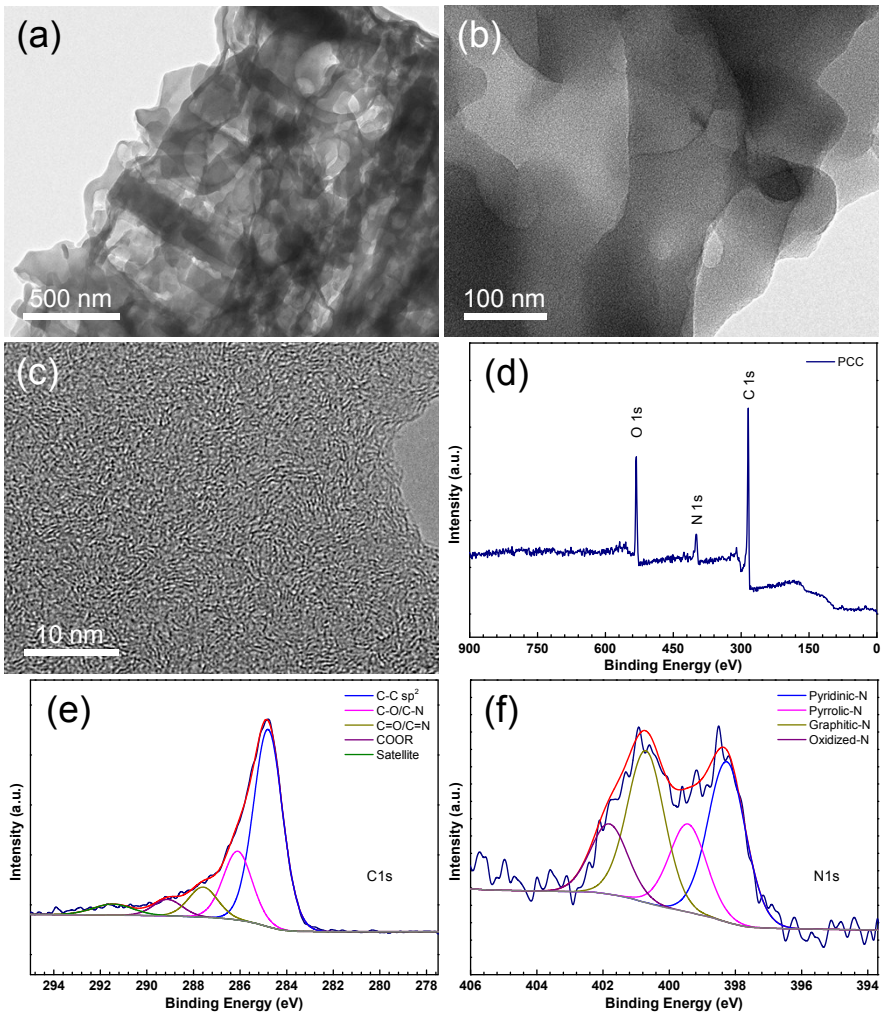

Figure S1. Morphology images and XPS spectra of the PCC sample. (a) and (b) TEM images; (c) high-resolution TEM image. (d) Full XPS spectrum containing C, O, and N; (e) high-resolution of C 1s spectrum, and (f) high-resolution of N 1s spectrum.

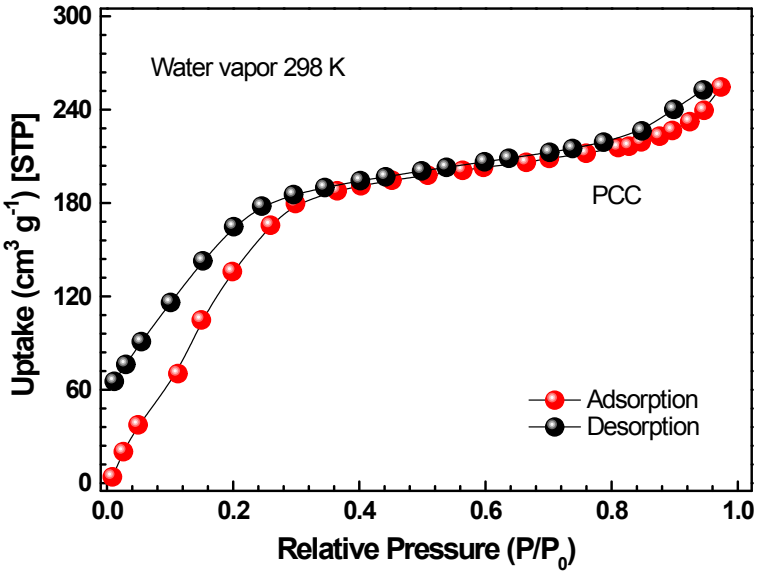

Figure S2. Water physisorption isotherms at 25 °C of the PCC sample.

The water physisorption isotherms show a sharp water capture until P/P_0=0.2, with a high uptake of 6.7 mmol g^{-1}. This outperforms the widely used commercial and well-studied carbons, which normally adsorb only a negligible amount of water at such low pressure.

Table S1. Elemental composition of as-prepared samples determined by energy dispersive X-ray spectroscopy.

Sample		Chemical Composition			
		C	N	O	Co
PCC	wt.%	64.52	21.77	13.71	-
	at.%	69.04	19.96	11.00	-
PCC-CoO_x	wt.%	63.09	12.40	8.46	16.05
	at.%	75.71	12.75	7.61	3.92

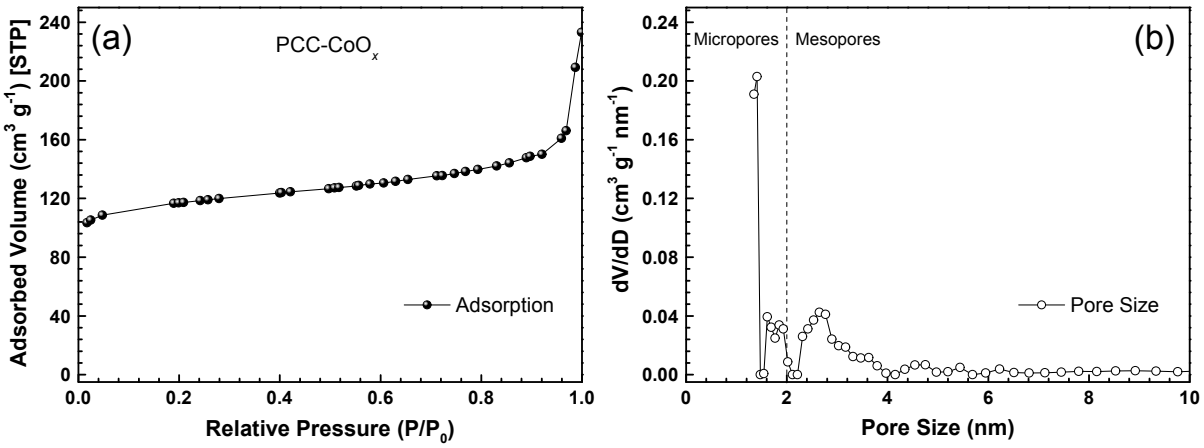

Figure S3. (a) Nitrogen physisorption isotherm, and (b) the corresponding pore size distribution curve obtained from the adsorption branch by applying non-local density functional theory (NLDFT) for the PCC-CoO_x sample.

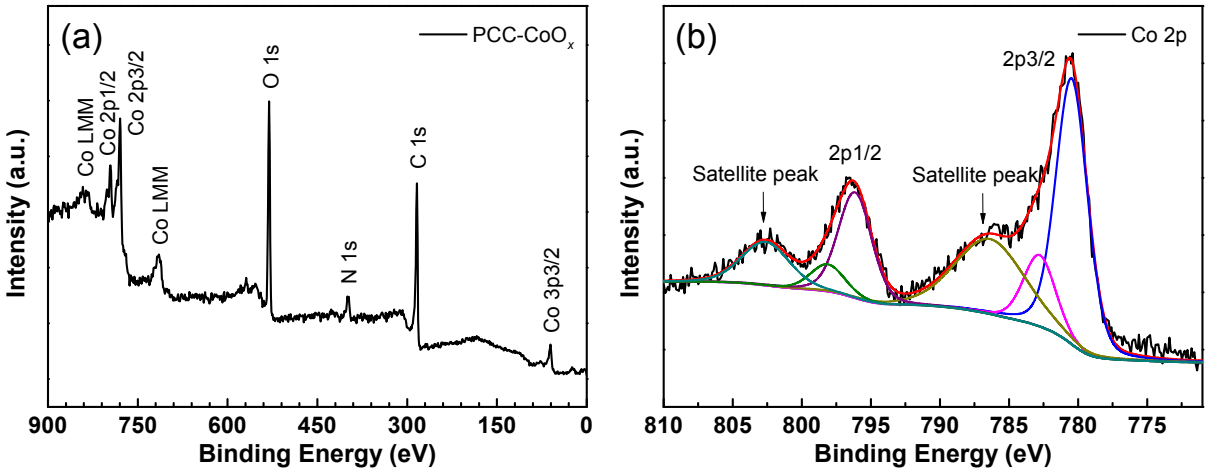

Figure S4. (a) Full XPS survey of the PCC-CoO_x sample containing C, Co, O, and N. (b) High-resolution of Co 2p spectrum (Co^0 and Co^{2+}).

Two relatively stronger satellite features with respect to Co 2p3/2 (782.8 eV) and Co 2p1/2 (798.1 eV) confirm the CoO pahse. Moreover, another two weak peaks around 780.4 and 796.1 eV also indicate the presence of metallic Co. Integral data show the molar ratio of Co/CoO is ~3.69. The results confirm the existence of CoO and metallic Co in the composite.

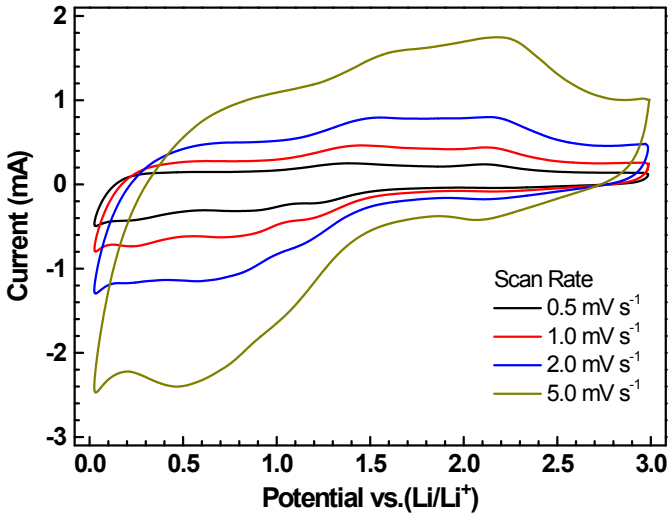

Figure S5. Cyclic voltammetry results for the PCC-CoO_x electrode at various sweep rates in the potential window of 0.01-3.0 V.

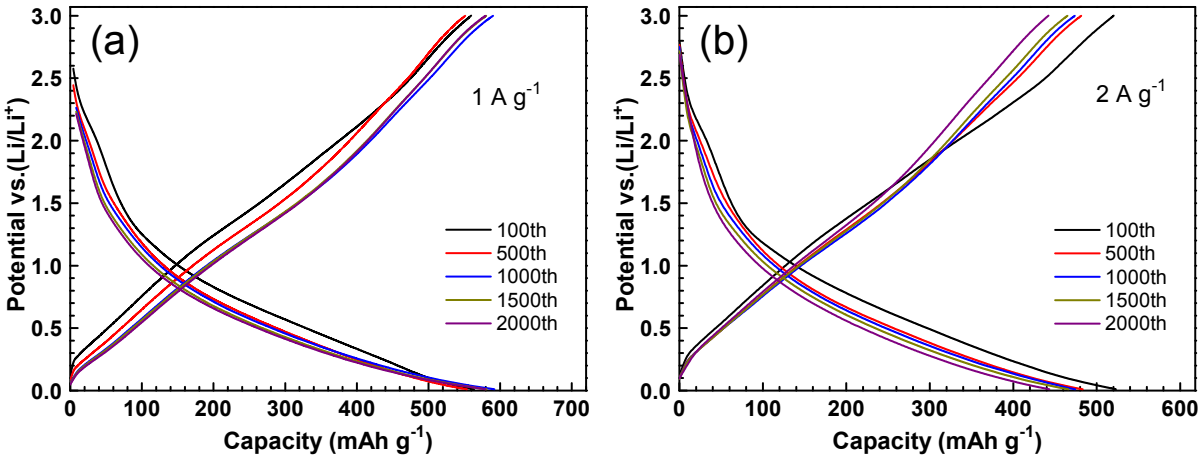

Figure S6. Discharge/charge voltage-capacity profiles of the PCC-CoO_x electrodes at (a) 1 A g^{-1} and (b) 2 A g^{-1}.

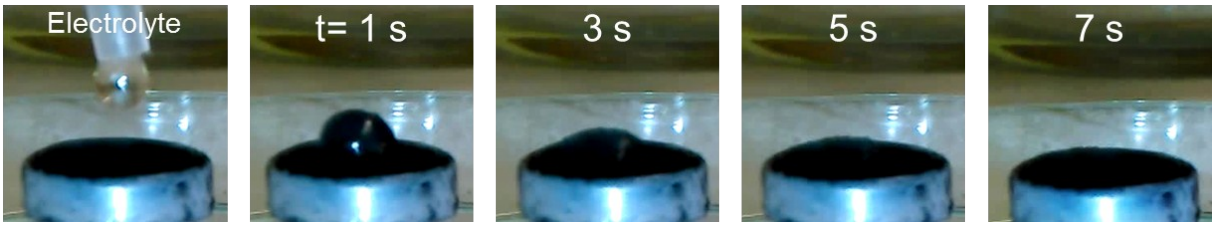

Figure S7. Time-lapse photographs of the electrolyte droplet (1.0 M $LiPF_6$ + EC/DEC/DMC) on the PCC-CoO_x sample.

Table S2. The comparison of the electrochemical performance of the PCC-CoO_x composite with the reported results.

Sample	Binder	Current Density (A g^{-1})	Cycle Number (times)	Capacity Retention (mAh g^{-1})	Reference
PCC-CoO_x cuboids	Na-alginate	5	10,000	301	**This work**
		2	2,000	442	
		1	2,000	580	
		0.5	500	618	
		0.1	20	1050*	
CoO octahedral nanocages	PVDF	0.14	50	807	[1]
CoO porous nanowire arrays	No binder	0.72	20	670	[2]
Mesoporous Co_3O_4 nanobelts	No binder	0.18	25	770	[3]
Double Co_3O_4 hollow spheres	PVDF	0.18	50	866	[4]
Needlelike Co_3O_4 nanotubes	PVDF	0.05	80	380	[5]
Graphene/CoO hybrids	No binder	1	5,000	604	[6]
	PVDF	1	2,000	256	
CoO@N-C nanocubes	PVDF	0.1	50	598	[7]
Peapod-like Co_3O_4@CNTs	PVDF	0.1	60	700	[8]
graphene/Co_3O_4 nanospheres	PVDF	1	500	600	[9]
Co_3O_4 nanowall@graphene	No binder	0.5	500	600	[10]
Graphene/Co_3O_4 nanoparticles	PVDF	0.05	30	935	[11]
Co_3O_4/graphene hybrids	PVDF	0.2	42	778	[12]
Porous $MnCo_2O_4$ microspheres	PVDF	0.2	25	755	[13]
$NiCo_2O_4$ microspheres	PVDF	0.8	500	705	[14]
$CoMoO_4$ nanoparticles/rGO	PVDF	0.74	600	600	[15]

$ZnCo_2O_4$ microspheres	CMC	5	2,000	550	[16]
Porous Fe_2O_3 nanosheets	No binder	2.01	1,000	877	[17]
	CMC	1	200	363	
Curved NiO nanomembranes	Na-alginate	1.08	1,400	721	[18]
MnO/carbon nanopeapods	PVDF	2	1,000	525	[19]
Mn_3O_4 octahedra	CMC	0.3	500	620	[20]
Mesoporous CuO	CMC	0.5	300	695	[21]
MoO_2/graphene	PVDF	2	70	408	[22]
ZnO@ZnO QDs/carbon	No binder	0.5	100	699	[23]
TiO_2(B) nanosheets	No binder	0.34	1,000	196	[24]
SnO_x/carbon nanohybrids	PVDF	0.5	200	608	[25]

* The data is derived from subsequent capacity retention after the 10,000 cycles at 5 A g^{-1}.

Binder: Polyvinylidene fluoride (PVDF); Carboxymethyl cellulose (CMC).

References

[1] H. Guan, X. Wang, H. Li, C. Zhi, T. Zhai, Y. Bando, D. Golberg, *Chem. Commun.* **2012**, *48*, 4878.

[2] J. Jiang, J. Liu, R. Ding, X. Ji, Y. Hu, X. Li, A. Hu, F. Wu, Z. Zhu, X. Huang, *J. Phys. Chem. C* **2010**, *114*, 929.

[3] Y. Wang, H. Xia, L. Lu, J. Lin, *ACS Nano* **2010**, *4*, 1425.

[4] X. Wang, X.-L. Wu, Y.-G. Guo, Y. Zhong, X. Cao, Y. Ma, J. Yao, *Adv. Funct. Mater.* **2010**, *20*, 1680.

[5] X. W. Lou, D. Deng, J. Y. Lee, J. Feng, L. A. Archer, *Adv. Mater.* **2008**, *20*, 258.

[6] X.-L. Huang, R.-Z. Wang, D. Xu, Z.-L. Wang, H.-G. Wang, J.-J. Xu, Z. Wu, Q.-C. Liu, Y. Zhang, X.-B. Zhang, *Adv. Funct. Mater.* **2013**, *23*, 4345.

[7] K. Xie, P. Wu, Y. Zhou, Y. Ye, H. Wang, Y. Tang, Y. Zhou, T. Lu, *ACS Appl. Mater. Interfaces* **2014**, *6*, 10602.

[8] D. Gu, W. Li, F. Wang, H. Bongard, B. Spliethoff, W. Schmidt, C. Weidenthaler, Y. Xia, D. Zhao, F. Schüth, *Angew. Chem. Int. Ed.* **2015**, *54*, 7060.

[9] H. Sun, X. Sun, T. Hu, M. Yu, F. Lu, J. Lian, *J. Phys. Chem. C* **2014**, *118*, 2263.

[10] L. Li, G. Zhou, X.-Y. Shan, S. Pei, F. Li, H.-M. Cheng, *J. Power Sources* **2014**, *255*, 52.

[11] Z.-S. Wu, W. Ren, L. Wen, L. Gao, J. Zhao, Z. Chen, G. Zhou, F. Li, H.-M. Cheng, *ACS Nano* **2010**, *4*, 3187.

[12] H. Kim, D.-H. Seo, S.-W. Kim, J. Kim, K. Kang, *Carbon* **2011**, *49*, 326.

[13] J. Li, S. Xiong, X. Li, Y. Qian, *Nanoscale* **2013**, *5*, 2045.

[14] J. Li, S. Xiong, Y. Liu, Z. Ju, Y. Qian, *ACS Appl. Mater. Interfaces* **2013**, *5*, 981.

[15] J. Yao, Y. Gong, S. Yang, P. Xiao, Y. Zhang, K. Keyshar, G. Ye, S. Ozden, R. Vajtai, P. M. Ajayan, *ACS Appl. Mater. Interfaces* **2014**, *6*, 20414.

[16] J. Bai, X. Li, G. Liu, Y. Qian, S. Xiong, *Adv. Funct. Mater.* **2014**, *24*, 3012.

[17] K. Cao, L. Jiao, H. Liu, Y. Liu, Y. Wang, Z. Guo, H. Yuan, *Adv. Energy Mater.* **2015**, *5*, 1570020.

[18] X. Sun, C. Yan, Y. Chen, W. Si, J. Deng, S. Oswald, L. Liu, O. G. Schmidt, *Adv. Energy Mater.* **2014**, *4*, 1300912.

[19] H. Jiang, Y. Hu, S. Guo, C. Yan, P. S. Lee, C. Li, *ACS Nano* **2014**, *8*, 6038.

[20] Q. Hao, J. Wang, C. Xu, *J. Mater. Chem. A* **2014**, *2*, 87.

[21] Z. Bai, Y. Zhang, Y. Zhang, C. Guo, B. Tang, *Electrochim. Acta* **2015**, *159*, 29.

[22] Y. Sun, X. Hu, W. Luo, Y. Huang, *ACS Nano* **2011**, *5*, 7100.

[23] G. Zhang, S. Hou, H. Zhang, W. Zeng, F. Yan, C. C. Li, H. Duan, *Adv. Mater.* **2015**, *27*, 2400.

[24] S. Liu, Z. Wang, C. Yu, H. B. Wu, G. Wang, Q. Dong, J. Qiu, A. Eychmüller, X. W. Lou, *Adv. Mater.* **2013**, *25*, 3462.

[25] X. Zhou, Z. Dai, S. Liu, J. Bao, Y.-G. Guo, *Adv. Mater.* **2014**, *26*, 3943.